Chitosan Hydrogels Crosslinked with Oxidized Sucrose for Antimicrobial Applications

Sayaka Fujita , Hijiri Takeda , Junki Noda , Haruki Wakamori , Hiroyuki Kono *

Posted Date: 4 September 2023

doi: 10.20944/preprints202309.0138.v1

Keywords: chitosan; oxidized sucrose; polysaccharide hydrogel; antimicrobial activities

Article

Chitosan Hydrogels Crosslinked with Oxidized Sucrose for Antimicrobial Applications

Sayaka Fujita [1], Hijiri Takeda [1], Junki Noda [1], Haruki Wakamori [1,2] and Hiroyuki Kono [1,*]

[1] Division of Applied chemistry and Biochemistry, National Institute of Technology, Tomakomai College, Nishikioka 443, Tomakomai, Hokkaido 059 1275, Japan; fujita@tomakomai-ct.ac.jp (S.F.), th23819@stu.tomakomai-ct.ac.jp (H.T.), junki.noda@ees.hokudai.ac.jp (J.N.); haruki.wakamori@agc.com (H.W.)

[2] Hokkaido Soda Co. Ltd., Numanohata 134-122, Tomakomai 059 1364, Japan

* Correspondence: kono@tomakomai-ct.ac.jp; Tel./Fax: +81-144-67-8036

Abstract: Oxidized sucrose (OS) reacts with amino group-containing polysaccharides, including chitosan, without catalyst, resulting in hydrogels entirely composed of carbohydrates. The presence of imine bonds with low structural stabilities and unreacted aldehydes in the structures of these hydrogels hinder their application as biomaterials. Therefore, herein, the chitosan hydrogels (CTSGs) obtained after the crosslinking of chitosan with OS were reduced using sodium borohydride to convert imine bonds to secondary amines and aldehydes to alcohols. Structures of CTSGs were comprehensively characterized by Fourier transform infrared and ^{13}C nuclear magnetic resonance spectroscopies, and results implied that the degree of crosslinking (CR) depended on the OS feed amount used during CTSG preparation. Properties of CTSGs were significantly dependent on CR; with an increase in CR, thermal stabilities and dynamic moduli of CTSGs increased, whereas their swelling properties decreased. CTSGs exhibited antimicrobial properties against the gram-negative bacterium *Escherichia coli*, and their performances were also dependent on CR. Results indicated the potentials of CTSGs completely based on carbohydrates as antimicrobial hydrogels for various medical and pharmaceutical applications. We believe that this study will contribute to the development of hydrogels for application in the food, medical, and pharmaceutical fields.

Keywords: chitosan; oxidized sucrose; polysaccharide hydrogel; antimicrobial activities

1. Introduction

In recent years, chitosan has attracted attention as a very useful green biopolymer. Chitosan is derived from chitin consisting of β-(1,4)-*N*-acetylglucosamine (GlcNAc) residues obtained from the shells of crabs, shrimps, and insects. It is a renewable polymer that is abundant in nature and the second highest produced polysaccharide after cellulose. Chitosan is achieved via alkaline deacetylation of chitin, its structure is composed of β-(1,4)-glucosamine (GlcN) residues and little or no GlcNAc residues, and it is the only naturally occurring cationic polysaccharide. Chitosan exhibits excellent biocompatibility, biodegradability, low immunogenicity, ecological safety, and non-toxicity [1,2]. The numerous amino groups on the chitosan backbone can be protonated at pH < 6.5 (pKa value of the amino group in chitosan is approximately 6.5), rendering chitosan behave as a polycation. As a polycation, chitosan demonstrates antimicrobial properties due to electrostatic interaction between the positive surface charges of the amino groups in GlcN and negatively charged microbial cell membranes [2]. These properties have facilitated the application of chitosan in food-related, medical, and pharmaceutical processes such as food preservation [3], disease control in agricultural crops [4], wound dressing [5], and skin care [6]. However, the practical applications of chitosan are limited by its inferior water solubility caused by inter- and intra-molecular hydrogen bonds and low mechanical strength arising from low crystallinity as compared to those of cellulose and chitin. For example, chitosan-based tissue engineering scaffolds can easily break and fail to support tissue engraftment. Additionally, chitosan films and membranes are brittle and not enough ductile, thereby fracturing during wound healing. Hydrogels [7], microparticles [8], three-dimensional (3D) porous sponges [9],

and blends of chitosan with other polymers [10] have been investigated to broaden the applications of chitosan.

Among them, hydrogels are 3D network structures of polymers with crosslinked molecular chains, which can absorb and retain water. The retained water does not leak out under pressure. Hydrogels contain extremely large amounts of water (>90%) and are also used as medical materials because their water content composition is similar to those of human tissues. For instance, they are employed as hemostatic and anti-adhesive agents for affected areas [11], drug delivery system (DDS) carriers [12], and tissue scaffolds for regenerative medicine [13]. In the preparation of chitosan-based hydrogels, glutaraldehyde [14], epichlorohydrin [15], and ethylene glycol diglycidyl ether [16] are commonly used as crosslinking agents. These materials are highly toxic, and the resulting hydrogels are unsuitable for biological applications. In contrast, genipin is a naturally occurring crosslinking agent; nevertheless, its high cost renders its sustainable use difficult for economic reasons [17]. Oxidized sucrose (OS) is a non-toxic and inexpensive crosslinking agent. It is obtained by the oxidation of sucrose with periodate and has a polar backbone structure comprising hydroxyl groups and glycosidic bonds; moreover, unlike glutaraldehyde and formaldehyde, OS is nonvolatile and not environmentally toxic [18]. Furthermore, *in vitro* cell culture studies of protein scaffolds prepared using OS have demonstrated the biocompatibility of OS, rendering it an environmentally friendly and safe crosslinking agent [19]. During the oxidation of sucrose, the C3–C4 bond of the fructose residue and C2–C3 or C3–C4 bond of the glucose residue are oxidatively cleaved. Thus, OS consists of four aldehydes. Via these four aldehyde moieties, it can crosslink polysaccharides such as starch [20] and proteins including collagen [21] and keratin [22].

Previously, we have fabricated a hydrogel of carboxymethyl chitosan (CMC) using OS as a crosslinking agent [23]. The reaction between the amino group of CMC and aldehyde moieties of OS occurred in an aqueous solution at room temperature without catalyst, and corresponding hydrogels were readily obtained. The obtained CMC hydrogels swelled in natural region and their absorbency is attributed to the osmotic pressure generated by the free sodium cations and the electrostatic repulsion between CMC molecular chains due to the presence of carboxylate anions. CMC hydrogels do not sufficiently swell in acidic regions where the protonation of amino groups occurs, and are not expected to exhibit antimicrobial activities. In this study, chitosan was crosslinked with OS to synthesize chitosan hydrogels (CTSGs). The use of chitosan instead of CMC could provide the hydrogels that swell in acidic regions and possess antimicrobial activities. Crosslinking between the amino groups of chitosan and OS formed imine bonds. Moreover, the aldehydes in OS that were not used in crosslinking were retained in the structures of CTSGs. The imine bond is structurally unstable and unreacted aldehyde may further react with the amino group of chitosan, changing the structures and properties of CTSGs, thereby preventing the application of CTSGs as biomaterials. Therefore, CTSGs were reduced using sodium borohydride ($NaBH_4$) to convert the imine bonds to secondary amines and aldehydes to alcohols. Structures, rheological and thermal properties, swelling behaviors, and antimicrobial activities of the resulting CTSGs were investigated. Furthermore, based on the data obtained via these analyses, the structure–function relationships of CTSGs were examined with the aim of contributing to the development of hydrogels for application in the food, medical, and pharmaceutical fields.

2. Results and Discussion

2.1. Preparation of CTSGs

Before the synthesis of CTSGs, OS was fabricated according to a previous study [23]. During the oxidation of sucrose with sodium periodate ($NaIO_4$), the C3–C4 bond of the fructose residue and C2–C3 or C3–C4 bond of the glucose residue were oxidatively cleaved, yielding a mixture containing two structures of OS (namely, OS(I) and OS(II)) (Figure 1). Composition of OS was determined to be 52 mol% OS(I) and 48 mol% OS(II) via quantitative ^{13}C nuclear magnetic resonance (NMR) spectroscopy. Considering that the prepared OS is a mixture of OS(I) and OS(II), the average molecular weight and aldehyde content of OS were evaluated (325 g mol^{-1} and 12.3 mmol g^{-1}), respectively.

Preprints (www.preprints.org) | NOT PEER-REVIEWED | Posted: 4 September 2023 doi:10.20944/preprints202309.0138.v1

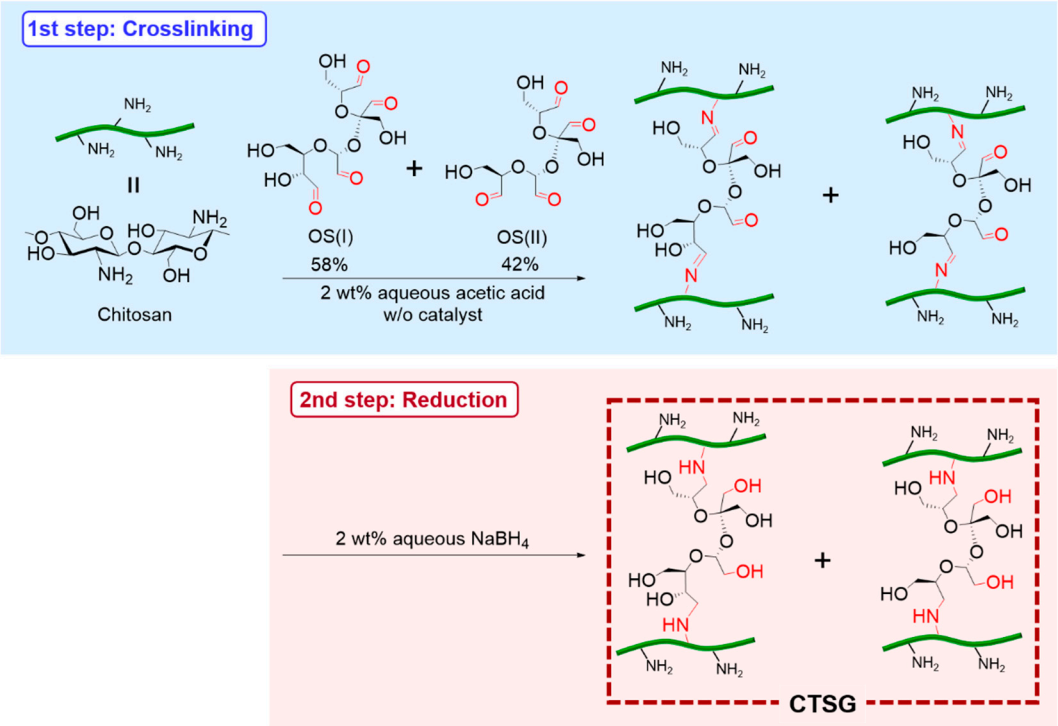

Figure 1. Preparation of chitosan hydrogels (CTSGs) using oxidized sucrose (OS) as a crosslinking agent. CTSGs were synthesized via two steps: crosslinking of chitosan with OS (top) and reduction of aldehydes and imines by $NaBH_4$ (bottom).

Subsequently, OS was used as a crosslinking agent to prepare CTSGs. CTSGs were fabricated via two steps: crosslinking and reduction (Figure 1). Crosslinking of chitosan was conducted using OS in aqueous acetic acid without catalyst at 298 K for 24 h (Figure 1 top). A series of three hydrogels (CTSG 1–3) (Table 1) were prepared by varying the initial OS:chitosan feed ratio. The four aldehyde groups of OS can react with the amine groups of chitosan to form imine bonds. Therefore, the molar aldehyde contents of OS were set to 0.2, 0.3, and 0.5 times those of the free amino groups of chitosan. Although the chitosan solution demonstrated no change immediately after the addition of OS, it became extensively viscous over time and morphology of the mixture gradually transformed from solution to gel. After 24 h of reaction, a clear yellow gel was acquired. The gel turned more yellowish with an increase in the feed amount of OS. CTSGs containing imine bonds formed using crosslinking agents, such as glutaraldehyde, are often yellowish and become more yellowish with an increase in the number of imine bonds [24,25]. Therefore, the change in the color of the gel with an increase in the feed amount of OS suggested an increase in the amount of OS in the gel. The yellow gel was crushed and employed for the second step, that is, reduction. The imine bonds produced by the crosslinking of chitosan with OS demonstrate low structural stabilities. The gel also comprises unreacted aldehydes that may further react with the amino groups of chitosan, thereby altering the structure and properties of CTSG. Additionally, if CTSG is used *in vivo*, unreacted aldehydes in CTSG can react with the amino groups of proteins, which hinders the application of CTSG as biomaterials. Thus, during reduction, the imine bonds and unreacted aldehyde moieties in the yellow gel were converted to secondary amines and alcohols, respectively. The crushed yellow gels were immersed in 2 wt% aqueous $NaBH_4$ for 24 h. The gels changed from yellow to colorless during reduction. The obtained CTSGs were purified by washing with water and subjected to dialysis to remove unreacted OS. Finally, lyophilization was performed to obtain CTSG 1–3 as white cotton-like hygroscopic solids.

Preprints (www.preprints.org) | NOT PEER-REVIEWED | Posted: 4 September 2023 doi:10.20944/preprints202309.0138.v1

Table 1. Initial feed amounts of chitosan and oxidized sucrose (OS) for the preparation of chitosan hydrogels (CTSG 1–3). Degrees of crosslinking (CRs) of CTSGs are also presented.

Sample	Initial feed amount		Feed mass ratio of Amine/Aldehyde	CR[a]	n_{OS}[b]
	chitosan (g) (Amine (mmol))	OS (g) (Aldehyde (mmol))			
CTSG 1	0.30 (1.9)	0.30 (0.4)	0.2	0.09	0.04
CTSG 2	0.30 (1.9)	0.45 (0.6)	0.3	0.14	0.06
CTSG 3	0.30 (1.9)	0.75 (0.9)	0.5	0.20	0.11

[a] Number of amine bonds formed between chitosan and OS per glucosamine residue. [b] Number of OS molecules reacted per glucosamine residue.

2.2. Structural Characterizations of CTSGs

Figure 2 shows the Fourier transform infrared (FTIR) spectra of CTSG 3 before and after reduction and the starting material chitosan. In the spectrum of chitosan, the broad absorption band at 3317 cm^{-1} corresponded to N–H and O–H stretching vibrations, and the absorption band at 2892 cm^{-1} was assigned to the C–H stretching vibration [26]. The characteristic absorption bands corresponding to the C=O stretching vibration (amide I) and N–H bending vibration (primary amine) were observed at 1644 and 1588 cm^{-1}, respectively [26]. Compared with the FTIR spectrum of chitosan, the FTIR spectrum of CTSG before reduction exhibited a new absorption band related to the C=N stretching vibration of the imine group (1635 cm^{-1}) [23,27] as a shoulder of amide I absorption band. This implied that the aldehyde groups of OS reacted with the amine groups of chitosan to form imine bonds. As the imine bonds were converted to amine moieties via reduction, the C=N absorption band should be absent in the spectrum of CTSG 3 after reduction. Nevertheless, this could not be clearly noticed due to the overlap of the imine absorption band with the amide I absorption band. FTIR spectrum of CTSG 3 after reduction demonstrated the absorption band of secondary amine at 1594 cm^{-1} [28], suggesting reduction of the imine bond to secondary amine. The absorption band of the aldehyde group (C=O stretching) was not observed at 1710 cm^{-1} [23,29] in the spectra of CTSG before and after reduction. The FTIR spectra did not clearly confirm the presence of aldehydes in CTSG and reduction of aldehydes.

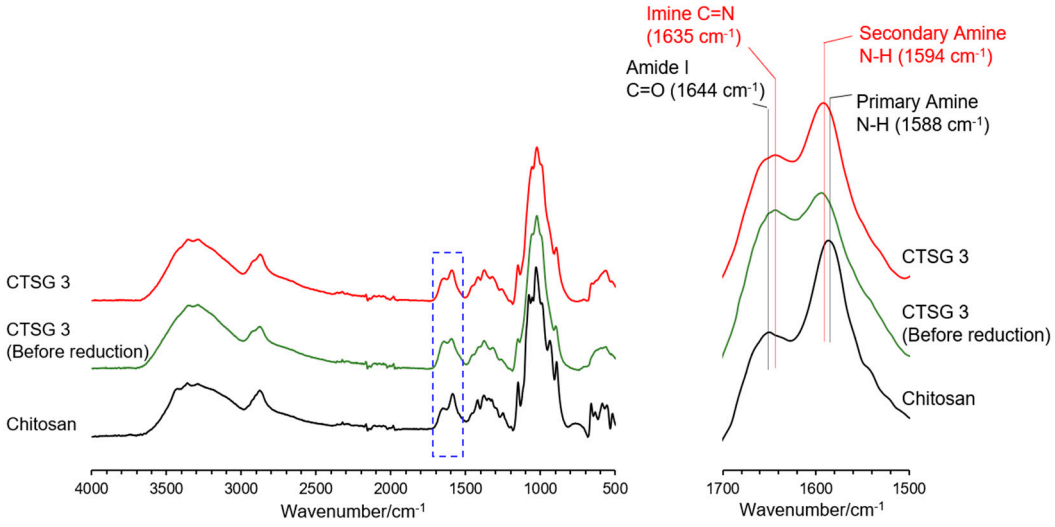

Figure 2. Full (left) and expanded (right) FTIR spectra of CTSG 3 before and after reduction and chitosan.

Figure 3 depicts the quantitative solid-state ^{13}C NMR spectra of CTSG 1–3 before and after reduction. In the NMR spectrum of chitosan, the broad resonances at 105, 87, 78, 63, and 56 ppm were attributed to the pyranose carbon C1, C4, overlap of C3 and C5, C6, and C2 in the chitosan backbone, respectively [30]. In the spectrum of OS, resonances of the carbon moieties of acetal, namely, CH and

Preprints (www.preprints.org) | NOT PEER-REVIEWED | Posted: 4 September 2023 doi:10.20944/preprints202309.0138.v1

CH_2, and the carbonyl carbons of the aldehyde groups were detected at 100–50 and 173 ppm, respectively. Compared with the spectrum of chitosan, the spectra of CTSGs exhibited new resonances at 168 and 173 ppm, which were assigned to imine carbons and carbonyl carbons of the aldehyde groups, respectively [23]. The existence of unreacted aldehydes and imines in the structures of CTSGs could not be distinctly verified via the FTIR spectra, whereas it was corroborated by the ^{13}C NMR spectra. These results indicated that OS reacted with the amino groups of chitosan. In the spectrum of CTSG after reduction, the resonances of the carbonyl carbons of the imine and aldehyde moieties were completely absent (Figure 3(b)), implying that the imine and aldehyde moieties were reduced to amine and alcohol moieties, respectively.

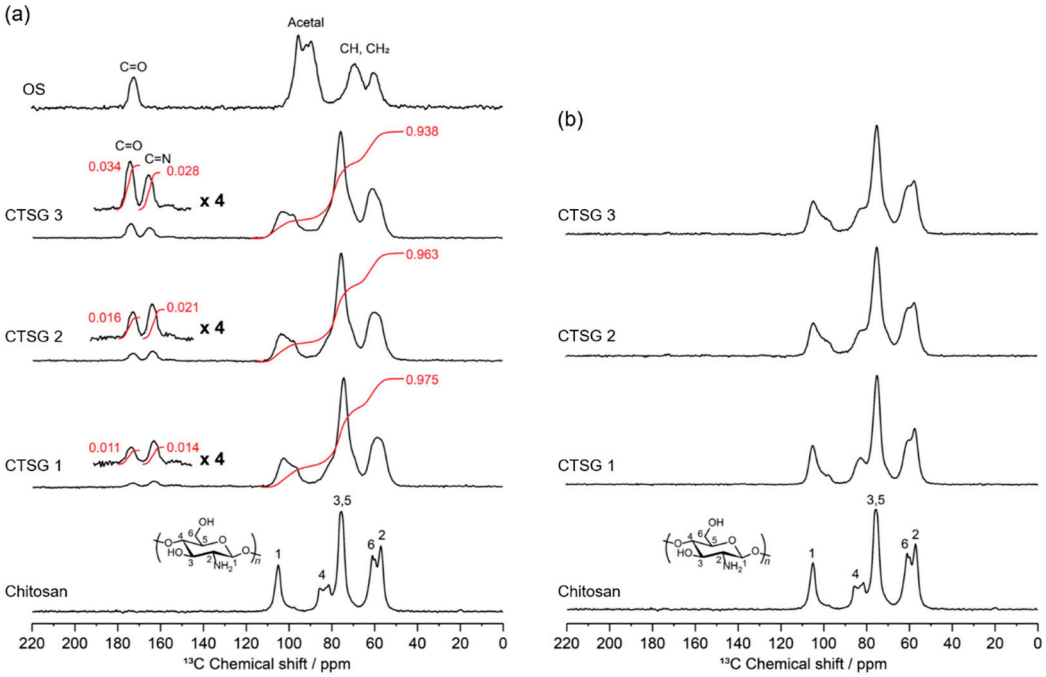

Figure 3. Quantitative solid-state ^{13}C NMR spectra of CTSG 1–3 (a) before and (b) after reduction. The spectra of chitosan and OS are also shown.

To estimate the amount of OS crosslinked to chitosan in CTSGs, the integral values of imine carbon ($I_{C=N}$), carbonyl carbon of aldehyde ($I_{C=O}$), and other carbon resonances (I_{others}) were determined (Figure 3(a)), and the sum of the integral values of all resonances was 1 ($I_{C=N} + I_{C=O} + I_{others} = 1$). Degrees of crosslinking (CRs) of CTSGs were calculated by speculating that OS introduced into chitosan was not dissociated by reduction. At first, the number of OS molecules reacted per glucosamine residue of chitosan (n_{OS}) was determined. The four aldehyde groups of OS reacted with chitosan to generate imine bonds, and CTSGs demonstrated four structures, as described hereinafter. Crosslinking between chitosan and OS resulted in CTSGs with two imine bonds and two unreacted aldehydes (Figure 1). The graft reaction led to the formation of one imine bond and three unreacted aldehydes. Moreover, a tri-bond with three imine bonds and one unreacted aldehyde and a tetra-bond with only four imine bonds can also produce; however, the probability of the generation of these bonds is substantially less than that of the formation of crosslinking and grafting bonds. In all these structures, the sum of the carbon atoms of aldehydes and imine carbon atoms in the OS linkage is always 4 and remains unchanged. Thus, the number of carbon atoms of aldehyde and imine in CTSG was $4n_{OS}$. Considering that the composition of OS is OS(I) and (II), OS used in crosslinking possesses an average of 11.6 carbon atoms per molecule, among which four carbon atoms are carbonyl carbons of aldehydes. Excluding the number of carbons of the aldehyde and imine groups, the number of carbons per OS-introduced glucosamine residue in CTSG was $6 + 7.6n_{OS}$. The relationship between n_{OS} and the integral values of resonances was established by Equation (1):

$$\frac{4n_{OS}}{6 + 7.6n_{OS}} = \frac{I_{C=O} + I_{C=N}}{I_{others}} \quad (1)$$

 doi:10.20944/preprints202309.0138.v1

CR of a CTSG is defined as the number of imine bonds (which are converted to amine bonds after reduction) formed between chitosan and OS per glucosamine residue and determined using Equation (2):

$$CR = 4n_{OS}\frac{I_{C=N}}{I_{C=O} + I_{C=N}} \quad (2)$$

The determined CR and n_{OS} for each CTSG are provided in Table 1. CRs and n_{OS} values for CTSG 1, 2, and 3 were 0.09, 0.14, and 0.20 and 0.04, 0.06, and 0.11, respectively. Clearly, CR and n_{OS} increased with an increase in the OS:chitosan feed ratio during CTSG synthesis. When one molecule of OS as a crosslinked structure was introduced into chitosan, the number of formed imine bonds was 2. That is, a CR:n_{OS} ratio of 2 indicates that the introduced OS is a crosslinked structure. CR:n_{OS} ratios for CTSG 1, 2, and 3 were 2.2, 2.3, and 1.8, respectively, which were close to 2. Thus, most of the reacted OS molecules were incorporated into the chitosan molecule as crosslinked structures.

2.3. Thermal Properties of CTSG

Figure 4a,b depicts thermogravimetric (TG)/differential thermogravimetric analysis (DTA) curves of CTSG 1–3 and chitosan. TG curve of chitosan demonstrated three weight-loss stages. During the first stage, a weight loss of approximately 11.5% occurred till 190 °C, attributed to vaporization of physically absorbed and intermolecular hydrogen-bonded water [31]. The second stage of weight loss took place in the range of 205–310 °C and was ascribed to depolymerization/decomposition of polymer chains and cleavage of glycosidic linkages [32]. The last stage of weight loss occurred at temperatures higher than 310 °C, corresponding to thermal destruction of pyranose ring and decomposition of residual carbon [33]. These thermal behaviors were confirmed by the presence of an endothermic peak at 67 °C and exothermic peaks at 298 and 380 °C in the DTA curve. TG curves of CTSG also demonstrated three weight-loss stages similar to those of chitosan.

Preprints (www.preprints.org) | NOT PEER-REVIEWED | Posted: 4 September 2023 doi:10.20944/preprints202309.0138.v1

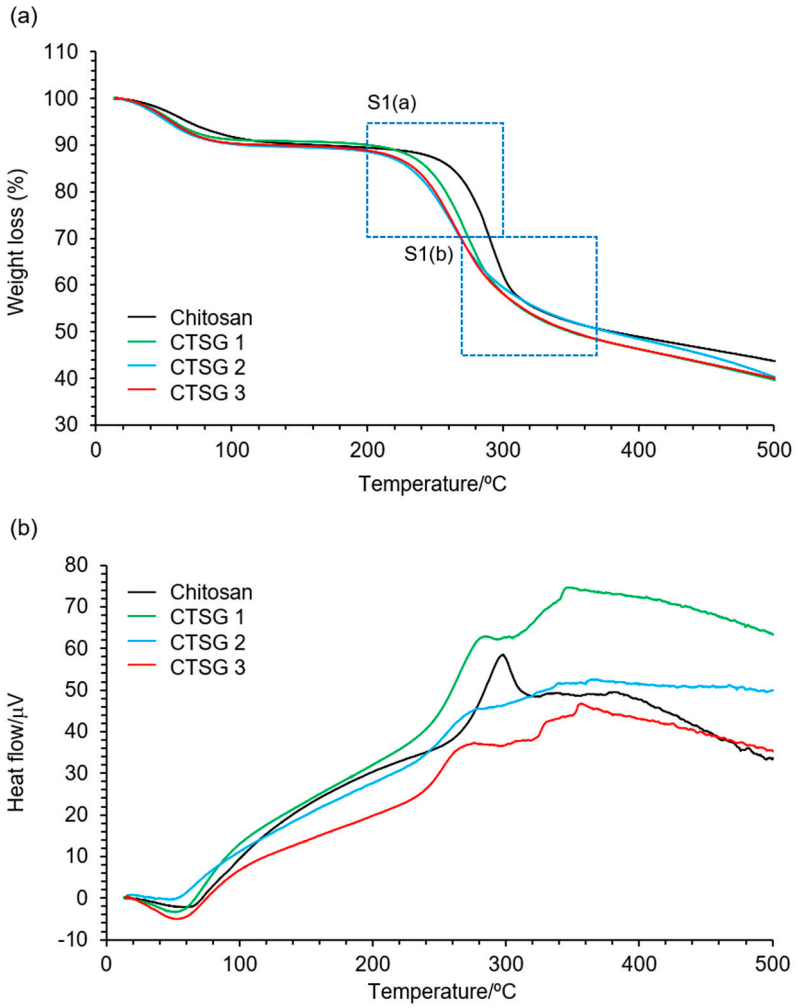

Figure 4. (a) Thermogravimetric (TG) and (b) differential thermogravimetric analysis (DTA) curves for CTSG 1–3 and chitosan. Magnified TG curves enclosed by dashed lines are shown in Figure S1(a) and (b).

Figure S1a,b shows the initial and final stages of the second stage of thermal decomposition. Initial (T_i) and final (T_f) decomposition temperatures for the second stage of degradation of chitosan and CTSG 1–3 are also depicted. T_i and T_f of chitosan were determined to be 264 and 308 °C, respectively. In the cases of CTSG 1–3, T_i values decreased and T_f values increased with an increase in CR. Generally, the incorporation of functional groups into polysaccharides causes the loss of interactions (for example, hydrogen bonding) between molecular chains, which decreases the thermal stabilities of polysaccharides [34,35]. The decrease in the T_i values of CTSG 1–3 was attributed to the decrease in the number of hydrogen bonds between molecular chains owing to the introduction of OS into the molecular chains of chitosan. The decrease in T_i with an increase in CR was explained by the loss of thermal stability of chitosan originating from hydrogen bonds upon the crosslinking of chitosan with OS. In contrast, the chemically crosslinked structures strengthened the molecular structures of CTSG 1–3 and increased the corresponding T_f values. This tendency was reported for a carboxymethyl chitosan hydrogel fabricated using OS as a crosslinking agent. In conclusion, the crosslinking of chitosan with OS decreased the interaction between the molecular chains of chitosan and resulted in CTSG 1–3 with high structural stabilities.

2.4. Water Absorbencies of CTSG 1–3 with Respect to pH

Images of swollen CTSG 1–3 in 20 mM acetate buffer (pH = 3) are shown in Figure 5a. When placed in acetic acid buffer, lyophilized CTSG 2 and 3 immediately absorbed water and turned

Preprints (www.preprints.org) | NOT PEER-REVIEWED | Posted: 4 September 2023 doi:10.20944/preprints202309.0138.v1

transparent, whereas CTSG 1 remained in the fluid state. Water absorbencies of CTSG 1–3 at pH = 3–6 are depicted in Figure 5b. At pH = 3, CTSG 1 was very fluid, CTSG 1 and unabsorbed excess solution could not be separated by centrifugation, and its water absorbency could not be determined. Except for the case of CTSG 1, water absorbencies of all CTSGs decreased with an increase in pH. Water absorbencies of chitosan-based hydrogels are caused by the protonation of the amino groups on the backbone of chitosan [36]. Under acidic conditions, as the dominant charged species in these hydrogels are protonated amino groups, the intermolecular network structure expands due to electrostatic repulsion between protonated amino groups, resulting in high water absorption. Under near natural conditions of pH = 5 and 6, the amino groups are deprotonated, the expansion of the network is suppressed, and water absorption is reduced. Water absorbencies of CTSG 2 and 3 decreased with an increase in CR. The highly crosslinked structures suppressed the expansions of chitosan molecules in CTSG 2 and 3, leading to lower water absorption.

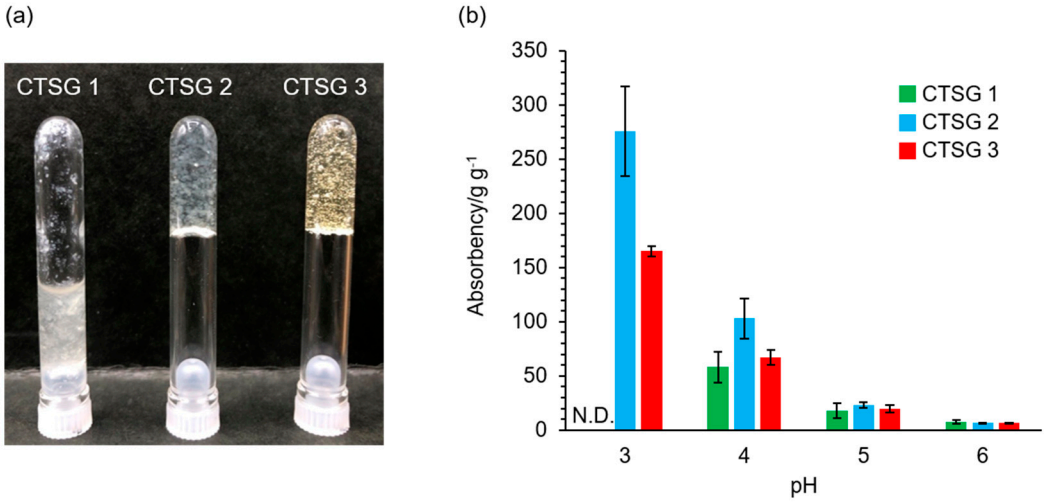

Figure 5. (a) Image showing swollen CTSG 1–3 in 20 mM acetate buffer (pH = 3). (b) Effects of pH on the absorbencies of CTSGs.

2.5. Rheological Properties of CTSGs

Figure 6 shows the plots of the storage (G′) and loss (G′′) moduli, tan δ, and complex viscosities (η^*) against the angular frequency sweeps for CTSGs swollen and saturated with acetate buffer with pH = 4. G′ values of all CTSGs were always higher than their G′′ values, and no crossover points (tan δ = 1) were noticed. tan δ values of CTSGs were in the range of 0.008–0.25, indicating that the elastic properties of CTSGs were superior to the viscous properties in the dynamic viscoelastic behaviors of CTSGs. For CTSG 2 and 3, the G′ and G′′ values were almost independent of the frequency characteristic of the permanent gel network. In contrast, the G′ and G′′ values of CTSG 1 exhibited drastic changes in the frequency dependence over 10 rad s^{-1}, implying that CTSG 1 exhibited the viscoelastic behavior of a weak gel [37]. Additionally, G′, G′′, and η^* increased with an increase in CR. These observations indicated that the viscoelastic behaviors of CTSGs were considerably dependent on CR and the addition of a large amount of OS to the reaction mixture to produce CTSGs significantly increased G′, G′′, and η^*.

Preprints (www.preprints.org) | NOT PEER-REVIEWED | Posted: 4 September 2023 doi:10.20944/preprints202309.0138.v1

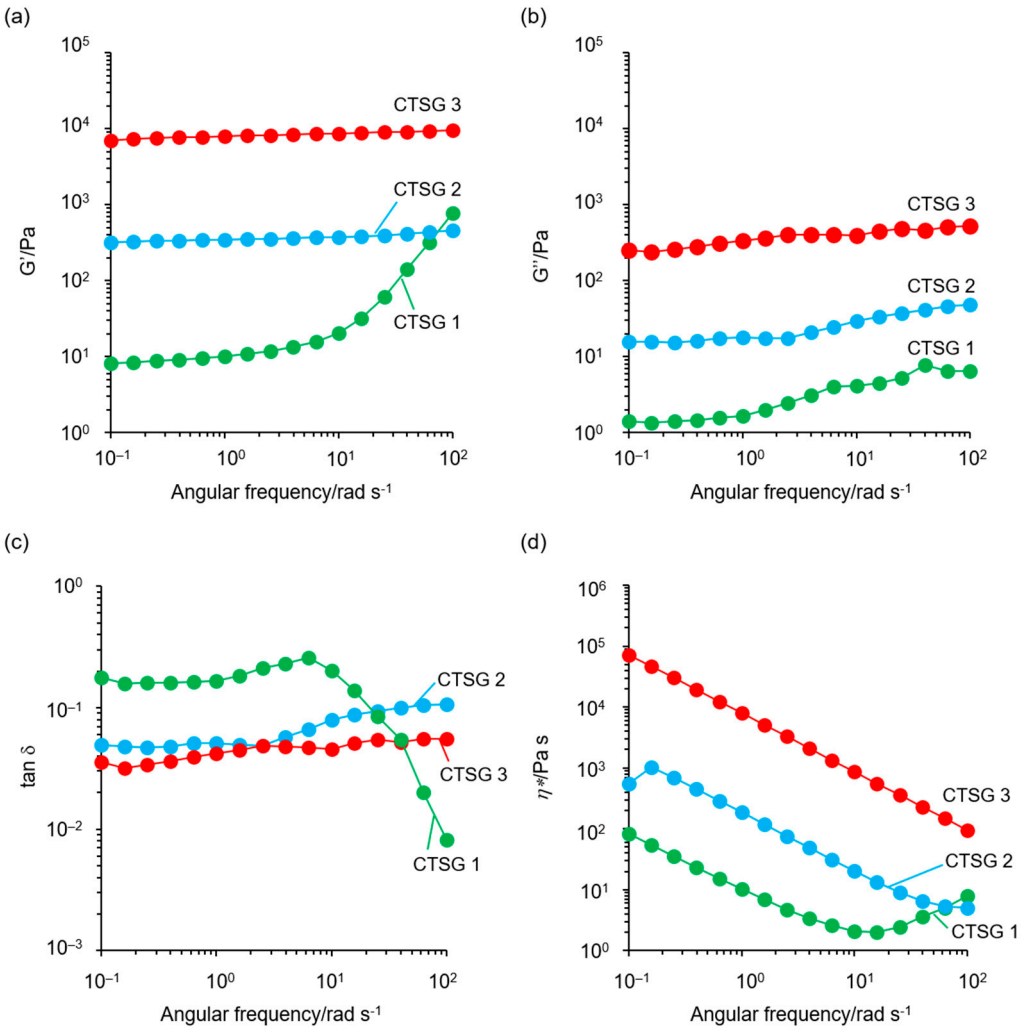

Figure 6. Rheological properties of CTSG 1–3 swollen and saturated with 20 mM acetate buffer (pH = 4) at 298 K: (a) storage modulus (G′), (b) loss modulus (G′′), (c) tan δ (= G′′/G′), and (d) complex viscosity (η^*).

2.6. Antimicrobial Activities of CTSGs

Antimicrobial activities of CTSGs against *Escherichia coli* (*E. coli*) were assessed by quantifying the number of colonies (colony-forming unit (CFU)/mL) of *E. coli* after the incubation of *E. coli* with CTSGs in Lysogeny Broth (LB) medium for 3 h (Figure 7). The cultured LB medium was incubated on standard method agar plates at 310 K for 24 h, and then, the number of colonies were counted. Incubations of *E. coli* with chitosan and without CTSGs were used as positive and negative controls, respectively. Compared with the case of the negative control, inhibitions of the growth of *E. coli* in the cases of chitosan and all CTSGs were statistically significant ($p < 0.001$). Several mechanisms for the inhibition of microbial growth by chitosan have been reported. The most appropriate mechanism is the interaction between the positive charge of chitosan and negatively charged membranes of microbial cells [38–40]. The amino groups on the chitosan backbone are protonated and positively charged. Positively charged amino groups (NH_3^+) interact with the negatively charged cell membranes of the microorganism via electrostatic forces resulting in antimicrobial effects. This interaction alters the permeability of the cell wall of the microorganism, disrupts the intracellular osmotic balance, and ultimately inhibits microbial growth. Moreover, this interaction causes hydrolysis of the peptidoglycans in the microbial wall. Consequently, intracellular electrolytes (for instance, Na and K ions) and various low-molecular-weight components (for example, lactate dehydrogenase, glucose, nucleic acids, and proteins) leak out. This prevents biosynthesis of the

Preprints (www.preprints.org) | NOT PEER-REVIEWED | Posted: 4 September 2023 doi:10.20944/preprints202309.0138.v1

microbial cell wall and blocks the transport of substances in and out of the cell wall, leading to antimicrobial activity. In the cases of CTSGs, the unreacted amino groups interacted with the membranes of microbial cells, resulting in antimicrobial effects.

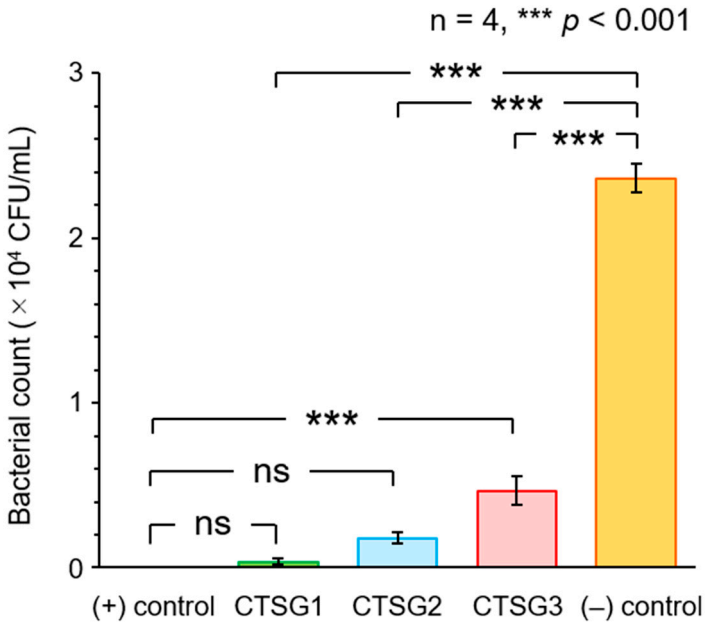

Figure 7. Antimicrobial activities of CTSG 1–3 against *Escherichia coli*, with chitosan and no sample as positive and negative controls, respectively. The columns and attached bars represent the means of the results of four identical samples and their standard errors. Asterisks and ns correspond to significant differences and non-significant difference between the results of the samples determined by statistical analysis (Tukey's test).

The number of colonies in the case of chitosan was 0 CFU/mL, suggesting complete inhibition of the growth of *E. coli*. In the cases of CTSGs, slight growth of *E. coli* was observed, which increased with an increase in CR. The decrease in the number of unreacted amino groups in CTSGs with an increase in CR weakened the interaction of CTSGs with the cell membranes of *E. coli*, resulting in low antimicrobial activities of CTSGs. The antimicrobial activities of CTSG 1 and 2 were not significantly different from that of chitosan, indicating that the antimicrobial properties of CTSGs with CRs of less than 0.14 were comparable to that of chitosan.

3. Conclusions

Herein, CTSGs were successfully synthesized by crosslinking chitosan with OS under an aqueous condition without catalyst. The imine bonds formed by the reaction of the amino groups in chitosan with OS and unreacted aldehydes were converted to secondary amines and alcohols, respectively, by immersing CTSGs in aqueous $NaBH_4$. CRs of CTSGs increased with an increase in the feed amount of OS during CTSG preparation. Thermal stabilities, dynamic moduli, and water absorbencies of CTSGs were considerably dependent on CR. CTSGs effectively inhibited the growth of *E. coli*, and their antimicrobial activities were dependent on CR. As CTSGs prepared in this study are composed of carbohydrates only, they can be applied in the food, medical, and pharmaceutical fields. For example, CTSGs can potentially be used as antimicrobial wound dressing gels; nevertheless, further research, for instance, on the biological safeties and antimicrobial activities of CTSGs against other microorganisms, is required in this regard. Additionally, the unreacted amino and hydroxyl groups of chitosan can be easily modified, endowing CTSGs with various functionalities such as drug loading and release capacities for application as DDS carriers [41] and antioxidant properties for application in food preservation [42].

 doi:10.20944/preprints202309.0138.v1

4. Materials and Methods

4.1. Materials

Chitosan (average molecular weight = 1 × 10^5 according to manufacturer's data) with a deacetylation degree of 100% was obtained from Dainichiseika Color & Chemicals Mfg. Co., Ltd. (Tokyo, Japan). Sucrose, sodium periodate, and barium chloride dihydrate were purchased from Fujifilm Wako Pure Chemical Co., Ltd. (Osaka, Japan). $NaBH_4$ was procured from Tokyo Chemical Industry Co., Ltd. (Tokyo, Japan). Acetate buffer was synthesized using analytical-grade sodium acetate and acetic acid purchased from Kanto Chemical Co., Inc. (Tokyo, Japan).

4.2. Preparation of OS

OS was fabricated by a previously described method [23]. Briefly, sucrose (6.0 g, 17.5 mmol) and sodium periodate (11.3 g, 52.5 mmol) were dissolved in deionized water (200 mL), and the resulting mixture was stirred at 298 K for 26 h. After the reaction, barium dichloride (6.42 g, 26.2 mmol) was added to the resulting mixture followed by stirring at 278 K for 1 h to allow complete precipitation of barium iodate. The resulting solution was filtered, and the supernatant solution was passed through a cation-exchange column filled with an anion-exchange resin (Amberlite FPC3500, Organo Co., Ltd., Tokyo, Japan) adjusted to the OH type followed by passing through a cation-exchange column filled with a cation-exchange resin (Amberlite IRA402BLCl, Organo Co., Ltd., Tokyo, Japan). OS was obtained as a white solid powder from the lyophilized solution.

Concentrations of OS(I) and OS(II) in OS were 52 and 48 mol%, respectively. The molecular formula of the OS mixture $(C_{12}H_{18}O_{11})_{0.52}$ $(C_{11}H_{16}O_{10})_{0.42}$ was $C_{11.58}$ $H_{17.16}$ $O_{15.58}$. The aldehyde content per unit mass of OS was 12.3 mmol g^{-1}.

4.3. Synthesis of CTSGs

Chitosan (0.3 g, 1.9 mmol of an average monomer unit) was completely dissolved in 2 wt% aqueous acetic acid (7.5 mL) followed by the addition of OS (30 mg) dissolved in deionized water (2.5 mL) under stirring at 298 K for 10 min. The reaction solution was allowed to stand at 298 K for 24 h to facilitate crosslinking. Then, the reaction mixture was crushed and soaked in 2 wt% aqueous $NaBH_4$ to reduce the formed imine bonds and unreacted aldehyde moieties. After leaving the reaction mixture in aqueous $NaBH_4$ for 24 h at 298 K, the resulting mixture was subjected to dialysis using a dialysis membrane tube with a molecular weight cutoff of 12,000 (Thermo Fisher Scientific, Massachusetts, USA) against deionized water followed by lyophilization to achieve CTSG 1. CTSGs with different chitosan and OS concentrations were prepared using a similar method (Table 1).

4.4. Structural Characterization

Attenuated total reflectance (ATR)-FTIR spectra were obtained using an ALPHA II FTIR spectrometer (Bruker Optics GmbH & Co., KG, Karlsruhe, Germany) at 295 K. To improve the signal-to-noise ratio for each spectrum, 32 interferograms with a spectral resolution of ±4 cm^{-1} were averaged. Background spectra, which were acquired under identical conditions, were subtracted from the sample spectra.

Solid-state cross-polarization/magic-angle spinning ^{13}C NMR (SSNMR) spectroscopy was performed at 298 K using an AVIII500 spectrometer (1H frequency of 500.13 MHz) equipped with a dual-tuned 4 mm magic-angle spinning probe (Bruker BioSpin GmbH, Karlsruhe, Germany). The sample (80 mg) was packed into a 4 mm ZrO_2 rotor, and the rotation frequency of the rotor was set to 10 kHz. The SSNMR spectra were obtained using ^{13}C-excitation pulse length (flip angle of 30°), and the data acquisition and repetition times were fixed at 1.5 μs, 20 ms, and 30 s, respectively. The ^{13}C chemical shifts were calibrated using the carboxyl carbon resonance of D-glycine (176.03 ppm) as an external standard.

4.5. TG/DTA

 doi:10.20944/preprints202309.0138.v1

TG/DTA curves were acquired via an EVO2 TG 8120 Plus thermogravimetric dynamic thermal analyzer (Rigaku Co., Tokyo, Japan) using an Al_2O_3 crucible under a nitrogen gas flow. Each sample weighed 15 mg, and the thermograms were obtained in the 50–500 °C temperature range at a heating rate of 5 °C min^{-1}.

4.6. Water absorbency

Water absorbencies were measured via gravimetric analysis. Each sample of a fixed weight was separately immersed in a large amount of acetate buffer with different pH values of 3, 4, and 5 at 298 K for 24 h. Thereafter, the swollen sample was centrifuged at 8000 x g for 10 min. The equilibrium water absorbency of the sample was determined using Equation (3):

$$\boldsymbol{Water\ absorbency} = \frac{m_2 - m_1}{m_1}, \quad (3)$$

where m_1 and m_2 are the weights of the samples in the dry and swollen states, respectively. All experiments were conducted in triplicate, and the results were averaged.

4.7. Rheological Measurements

Rheological behavior of each sample swollen in phosphate buffered saline at 298 K for 24 h was evaluated in triplicate using a Physica MCR 301 rheometer (Anton Paar GmbH, Graz, Austria) equipped with a 25 mm parallel-plate measuring geometry, Peltier device for temperature control, and Rheoplus 32 data analyzer. The gap and strain were set to 1.0 mm and 0.5%, respectively. Oscillatory shear responses at 298 K were determined under 0.1 Pa over the frequency range of steady shear tests with an angular frequency range of 10^{-1}–10^{2} rad·s^{-1}.

4.8. Determination of Antimicrobial Activities

E. coli NBRC3301 cultured on standard method agar plates (Nissui Pharmaceutical Co., Ltd., Tokyo, Japan; Composition: 0.25 w/v% yeast extract, 0.5 w/v% peptone, 0.1 w/v% glucose, and 1.5 w/v% agar) at 310 K was used to evaluate the antimicrobial activities of CTSGs. The single colony was cultured in LB medium (MP Biomedicals, California, USA; Composition: 1.0 w/v% tryptone, 0.5 w/v% yeast extract, and 1.0 w/v% NaCl) for 24 h at 310 K, and the resulting colonies were suspended in saline solution (Otsuka Pharmaceutical Factory, Inc., Tokushima, Japan) to achieve an optical density at 600 nm (OD_{600}) of ca. 0.2. The suspension diluted 10^3-fold in fresh LB medium (1 mL) was separately added to a 24-well microplate containing CTSGs (20 mg dry weight), neat chitosan as a positive control, and no sample as a negative control. The bacterial culture was used at a concentration of 0.38×10^4 CFU/mL, which was determined by counting the number of colonies after the incubation of the bacterial suspension on a standard method agar plate at 310 K for 24 h. After incubation at 310 K for 3 h, the supernatant of the culture medium (0.1 mL) was diluted 10-fold with saline solution and then cultured on the standard method agar plate at 310 K for 24 h. Antimicrobial activities of the samples were determined by counting the number of colonies on the plate. Values are presented as the mean of the results of three identical samples (n = 4). Statistical analyses were performed by Tukey's test using analysis of variance with R (EZR version 1.61, Jichi Medical University, Saitama, Japan) [43].

Supplementary Materials: The following supporting information can be downloaded at the website of this paper posted on Preprints.org., Figure S1: (a) Initial (T_i) and (b) final (T_f) degradation temperatures for the second degradation of CTSG 1–3 and chitosan determined by thermogravimetric analysis.

Author Contributions: Conceptualization, H.K.; methodology, S.F., H.T., J.N., H.W., and H.K.; validation, S.F., H.T., J.N., and H.K.; formal analysis, H.T., J.N., and H.K.; investigation, S.F., H.T., J.N., H.W., and H.K.; data curation, S.F., H.T., H.W., and H.K.; writing—original draft preparation, S.F. and H.K.; writing—review and editing, H.K.; visualization, S.F.; supervision, H.K.; project administration, H.K.; funding acquisition, S.F. and H.K. All authors read and agreed to the published version of the manuscript.

Funding: This research was partially funded by the JAPAN SOCIETY FOR THE PROMOTION OF SCIENCE (JSPS) KAKENHI, grant number JP21K14664 (S.F.) and JP21K05175 (H.K.), and JST SATREPS, grant number JPMJSA2206.

Institutional Review Board Statement: Not applicable.

Informed Consent Statement: Not applicable.

Data Availability Statement: The data presented in this study, supporting the results, are available in the main text. Additional data are available upon request from the corresponding authors.

Conflicts of Interest: The authors declare no conflict of interest.

References

1. Lv, S.; Zhang, S.; Zuo, J.; Liang, S.; Yang, J.; Wang, J.; Wei, D. Progress in preparation and properties of chitosan-based hydrogels. *Int. J. Biol. Macromol.* **2023**, *242*, 124915. doi.org/10.1016/j.ijbiomac.2023.124915
2. Guarnieri, A.; Triunfo, M.; Scieuzo, C.; Ianniciello, D.; Tafi, E.; Hahn, T.; Zibek, S.; Salvia, R.; Bonis, A.D.; Falabella, P. Antimicrobial properties of chitosan from different developmental stages of the bioconverter insect *Hermetia illucens*. *Sci. Rep.* **2022,** 2, 8084. doi.org/10.1038/s41598-022-12150-3
3. Duan, C.; Meng, X.; Meng, J.; Khan, M.I.H.; Dai, L.; Khan, A.; An, X.; Zhang, J.; Huq, T.; Ni, Y. Chitosan as a preservative for fruits and vegetables: A review on chemistry and antimicrobial properties. *J. Bioresour. Bioprod.* **2019**, *4*, 11–21. doi.org/10.21967/jbb.v4i1.189
4. Maluin, F.N.; Hussein, M.Z. Chitosan-based agronanochemicals as a sustainable alternative in crop protection. *Molecules* **2020**, 25, 1611. doi.org/10.3390/molecules25071611
5. Moeini, A.; Pedram, P.; Makvandi, P.; Malinconico, M.; d'Ayala, G.G. Wound healing and antimicrobial effect of active secondary metabolites in chitosan-based wound dressings: A review. *Carbohydr. Polym.* **2020**, *233*, 115839. doi.org/10.1016/j.carbpol.2020.115839
6. Aranaz, I.; Acosta, N.; Civera, C.; Elorza, B.; Mingo, J.; Castro, C.; Gandía, M.D.I.L.; Heras Caballero, A. Cosmetics and cosmeceutical applications of chitin, chitosan and their derivatives. *Polymers* **2018**, *10*, 213. https://doi.org/10.3390/polym10020213
7. Zhang, X.; Qin, M.; Xu, M.; Miao, F.; Merzougui, C.; Zhang, X.; Wei, Y.; Chen, W.; Huang, D. The fabrication of antibacterial hydrogels for wound healing. *Eur. Polym. J.* **2021**, *146*, 110268. doi.org/10.1016/j.eurpolymj.2021.110268
8. Lin, P.; Zhang, W.; Chen, D; Yang, Y.; Sun, T.; Chen, H.; Zhang, J. Electrospun nanofibers containing chitosan-stabilized bovine serum albumin nanoparticles for bone regeneration. *Colloids Surf. B* **2022**, *217*, 112680. doi.org/10.1016/j. colsurfb.2022.112680
9. Sukpaita, T.; Chirachanchai, S.; Pimkhaokham, A.; Ampornaramveth, R.S. Chitosan-based scaffold for mineralized tissues regeneration. *Mar. Drugs* **2021**, *19*, 551. doi.org/10.3390/md19100551
10. Kalaycıoğlu, Z.; Kahya, N.; Adımcılar, V.; Kaygusuz, H.; Torlak, E.; Akın-Evingür, G.; Erim, F.B. Antibacterial nano cerium oxide/chitosan/cellulose acetate composite films as potential wound dressing. *Eur. Polym. J.* **2020**, *133*, 109777. doi.org/10.1016/j.eurpolymj.2020.109777
11. Hu, Z.; Zhang, D.-Y.; Lu, S.-T.; Li, P.-W.; Li, S.-D. Chitosan-based composite materials for prospective hemostatic applications. *Mar. Drugs* **2018**, *16*, 273. doi.org/10.3390/md16080273
12. Kesharwani, P.; Bisht, A.; Alexander, A.; Dave, V.; Sharma, S. Biomedical applications of hydrogels in drug delivery system: An update. *J. Drug Deliv. Sci. Technol.* **2021**, 66, 102914. doi.org/10.1016/j.jddst.2021.102914
13. Sultankulov, B.; Berillo, D.; Sultankulova, K.; Tokay, T.; Saparov, A. Progress in the development of chitosan-based biomaterials for tissue engineering and regenerative medicine. *Biomolecules* **2019**, *9*, 470. doi.org/10.3390/biom9090470
14. Yu, S.; Zhang, X.; Tan, G.; Tian, L.; Liu, D.; Liu, Y.; Yang, X.; Pan, W. A novel pH-induced thermosensitive hydrogel composed of carboxymethyl chitosan and poloxamer cross-linked by glutaraldehyde for ophthalmic drug delivery. *Carbohydr. Polym.* **2017**, *155*, 208–217. doi.org/10.1016/j.carbpol.2016.08.073
15. Zhu, H.; Chen, S.; Duan, H.; He, J.; Luo, Y. Removal of anionic and cationic dyes using porous chitosan/carboxymethyl cellulose-PEG hydrogels: optimization, adsorption kinetics, isotherm and thermodynamics studies. *Int. j. Biol. Macromol.* **2023**, 231, 123213. doi.org/10.1016/j.ijbiomac.2023.123213
16. Bratskaya, S.; Privar, Y.; Nesterov, D; Modin, E.; Kodess, M.; Slobodyuk, A.; Marinin, D.; Pestov, A. Chitosan gels and cryogels cross-linked with diglycidyl ethers of ethylene glycol and polyethylene glycol in acidic media. *Biomacromolecules* **2019**, *20*, 1635–1643. doi.org/10.1021/acs.biomac.8b01817
17. Muzzarelli, R.A.A.; El Mehtedi, M.; Bottegoni, C.; Aquili, A.; Gigante, A. Genipin-crosslinked chitosan gels and scaffolds for tissue engineering and regeneration of cartilage and bone. *Mar. Drugs* **2015**, *13*, 7314–7338. doi.org/10.3390/md13127068
18. Xu, H.; Canisag, H.; Mu, B.; Yang, Y. Robust and flexible films from 100% starch cross-linked by biobased disaccharide derivative. *ACS Sustain. Chem. Eng.* **2015**, *3*, 2631–2639. doi.org/10.1021/acssuschemeng.5b00353

19. Xu, H.; Liu, P.; Mi, X.; Xu, L.; Yang, Y. Potent and regularizable crosslinking of ultrafine fibrous protein scaffolds for tissue engineering using a cytocompatible disaccharide derivative. *J. Mater. Chem. B* **2015**, *3*, 3609–3616. doi.org/10.1039/C4TB02100B
20. Wang, P.; Sheng, F.; Tang, S.W.; ud-Din, Z.; Chen, L.; Nawaz, A.; Hu, C.; Xiong, H. Synthesis and characterization of corn starch crosslinked with oxidized sucrose. *Starch* **2019**, *71*, 1800152. doi.org/10.1002/star.201800152
21. El-Feky, G.S.; Zayed, G.M.; Elshaier, Y.A.M.M.; Alsharif, F.M. Chitosan-gelatin hydrogel crosslinked with oxidized sucrose for the ocular delivery of timolol maleate. *J. Pharma. Sci*. **2018**, *107*, 3098–3104. doi.org/10.1016/j.xphs.2018.08.015
22. Mi, X.; Chang, Y.; Xu, H.; Yang, Y. Valorization of keratin from food wastes via crosslinking using non-toxic oligosaccharide derivatives. *Food Chem*. **2019**, *300*, 125181. doi.org/10.1016/j.foodchem.2019.125181
23. Kono, H.; Noda, J.; Wakamori, H. Detailed structural characterization of oxidized sucrose and its application in the fully carbohydrate-based preparation of a hydrogel from carboxymethyl chitosan. *Molecules* **2022**, *27*, 6137. doi.org/10.3390/molecules27186137
24. Aguanell, A.; del Pozo, M.L.; Pérez-Martín, C.; Pontes, G.; Bastida, A.; Fernández-Mayoralas, A.; García-Junceda, E.; Revuelta, J. Chitosan sulfate-lysozyme hybrid hydrogels as platforms with fine-tuned degradability and sustained inherent antibiotic and antioxidant activities. *Carbohydr. Polym.* **2022**, *291*, 119611. doi.org/10.1016/j.carbpol.2022.119611
25. Luo, W.; Bai, Z.; Zhu, Y. Fast removal of Co(II) from aqueous solution using porous carboxymethyl chitosan beads and its adsorption mechanism. *RSC Adv*. **2018**, *8*, 13370–13387. doi.org/10.1039/C7RA13064C
26. Fujita, S.; Sakairi, N. Water soluble EDTA-linked chitosan as a zwitterionic flocculant for pH sensitive removal of Cu(ii) ion. *RSC Adv*. **2016**, 6, 10385–10392. doi.org/10.1039/c5ra24175h
27. Islam, N.; Wang, H.; Maqbool, F.; Ferro, V. In vitro enzymatic digestibility of glutaraldehyde-crosslinked chitosan nanoparticles in lysozyme solution and their applicability in pulmonary drug delivery. *Molecules* **2019**, 24, 1271. doi.org/10.3390/molecules24071271
28. Pawlak, A.; Mucha, M. Thermogravimetric and FTIR studies of chitosan blends. *Thermochim. Acta* **2003**, 396, 153–166. doi.org/10.1016/S0040-6031(02)00523-3
29. Feng, M.; Hu, X.; Yin, Y.; Liang, Y.; Niu, J.; Yao, J. Structural analysis of oxidized sucrose and its application as a crease-resistant crosslinking agent. *Polymers* **2022**, *14*, 2842. doi.org/10.3390/polym14142842
30. Kono, H.; Oeda, I.; Nakamura, T. The preparation, swelling characteristics, and albumin adsorption and release behaviors of a novel chitosan-based polyampholyte hydrogel. *React. Funct. Polym*. **2013**, *73*, 97–107. doi.org/10.1016/j.reactfunctpolym.2012.08.016
31. Kraskouski, A.; Hileuskaya, K.; Nikalaichuk, V.; Ladutska, A.; Kabanava, V.; Yao, W.; You, L. Chitosan-based Maillard self-reaction products: Formation, characterization, antioxidant and antimicrobial potential. *Carbohydr. Polym. Technol. Appl.* **2022**, *4*, 100257. doi.org/10.1016/j.carpta.2022.100257
32. Moussout, H.; Ahlafi, H.; Aazza, M.; Bourakhouadar, M. Kinetics and mechanism of the thermal degradation of biopolymers chitin and chitosan using thermogravimetric analysis. *Polym. Degrad. Stab.* **2016**, *130*, 1–9. doi.org/10.1016/j.polymdegradstab.2016.05.016
33. Bayazit, N.; Cakran, H.S.; Çabir, A.; Akışcan, Y.; Demetgül, C. Synthesis, characterization and antioxidant activity of chitosan Schiff base derivatives bearing (−)-gossypol. *Carbohydr. Polym*. **2020**, *240*, 116333. doi.org/10.1016/j.carbpol.2020.116333
34. Zong, Z.; Kimura, Y.; Takahashi, M.; Yamane, H. Characterization of chemical and solid state structures of acylated chitosans. *Polymer* **2000**, *41*, 899–906. doi.org/10.1016/S0032-3861(99)00270-0
35. Ma, G.; Yang, D.; Zhou, Y.; Xiao, M.; Kenn, J.F.; Nie, J. Preparation and characterization of water-soluble *N*-alkylated chitosan. *Carbohydr. Polym.* **2008**, *74*, 121–126. doi.org/10.1016/j.carbpol.2008.01.028
36. Abd El-Hady, M.M.; Saeed, S.E.-S. Antibacterial properties and pH sensitive swelling of insitu formed silver-curcumin nanocomposite based chitosan hydrogel. *Polymers* **2020**, *12*, 2451. doi.org/10.3390/polym12112451
37. Kono, H. Carboxymethyl cellulose-based hydrogels. In *Cellulose and Cellulose Derivatives: Synthesis, Modification and Applications*, 1st ed.; Mondal, M.I.H., Ed.; Nova Science Publishers Inc.: New York, NY, USA, 2015; pp. 243–258.
38. Li, J.; Zhao, L.; Wu, Y.; Rajoka, M.S.R. Insights on the ultra high antibacterial activity of positionally substituted 2′-O-hydroxypropyl trimethyl ammonium chloride chitosan: A joint interaction of -NH_2 and -$N^+(CH_3)_3$ with bacterial cell wall. *Colloids Surf. B* **2019**, *173*, 429–436. doi.org/10.1016/j.colsurfb.2018.09.077
39. Yu, Q.; Yan, Y.; Huang, J.; Liang, Q.; Li, J.; Wang, B.; Ma, B.; Bianco, A.; Ge, S.; Shao, J. A multifunctional chitosan-based hydrogel with self-healing, antibacterial, and immunomodulatory effects as wound dressing. *Int. J. Biol. Macromol.* **2023**, *231*, 123149. doi.org/10.1016/j.ijbiomac.2023.123149
40. Tang, H.; Zhang, P.; Kieft, T.L.; Ryan, S.J.; Baker, S.M.; Wiesmann, W.P.; Rogelj, S. Antibacterial action of a novel functionalized chitosan-arginine against Gram-negative bacteria. *Acta Biomater.* **2010**, *6*, 2562–2571. doi.org/10.1016/j.actbio.2010.01.002

41. Kono, H.; Teshirogi, T. Cyclodextrin-grafted chitosan hydrogels for controlled drug delivery. *Int. J. Biol. Macromol.* **2015**, *72*, 299–308. doi.org/10.1016/j.ijbiomac.2014.08.030
42. Yang, X.; Lan, W.; Sun, X. Antibacterial and antioxidant properties of phenolic acid grafted chitosan and its application in food preservation: A review. *Food Chem.* **2023**, *428*, 136788. doi.org/10.1016/j.foodchem.2023.136788
43. Kanda, Y. Investigation of the freely available easy-to-use software 'EZR' for medical statistics. *Bone Marrow Transplant.* **2013**, *48*, 452–458. doi.org/10.1038/bmt.2012.244